Fourier methods for the perturbed harmonic oscillator in linear and nonlinear Schrödinger equations

Philipp Bader* and Sergio Blanes†

Universitat Politècnica de València, Instituto de Matemática Multidisciplinar, E-46022 Valencia, Spain

(Received 20 July 2010; revised manuscript received 28 February 2011; published 29 April 2011)

We consider the numerical integration of the Gross-Pitaevskii equation with a potential trap given by a time-dependent harmonic potential or a small perturbation thereof. Splitting methods are frequently used with Fourier techniques since the system can be split into the kinetic and remaining part, and each part can be solved efficiently using fast Fourier transforms. Splitting the system into the quantum harmonic-oscillator problem and the remaining part allows us to get higher accuracies in many cases, but it requires us to change between Hermite basis functions and the coordinate space, and this is not efficient for time-dependent frequencies or strong nonlinearities. We show how to build methods that combine the advantages of using Fourier methods while solving the time-dependent harmonic oscillator exactly (or with a high accuracy by using a Magnus integrator and an appropriate decomposition).

DOI: 10.1103/PhysRevE.83.046711 PACS number(s): 02.60.Cb, 02.60.Lj, 02.70.Hm

I. INTRODUCTION

The numerical integration of the Gross-Pitaevskii equation (GPE),

$$i\frac{\partial}{\partial t}\psi(x,t) = \left(-\frac{1}{2\mu}\Delta + V(x,t) + \sigma(t)|\psi(x,t)|^2\right)\psi(x,t),$$

$x \in \mathbb{R}^d$, describing the ground state of interacting bosons at zero temperature (the Bose-Einstein condensates), has attracted a great deal of interest [1–3] after the initial experimental realizations [4]. We present an efficient way to solve a special class of GPE, namely that of weakly interacting bosons in a single time-dependent trap. To be more specific, the potential trap V is taken to be a perturbation of the (time-dependent) d-dimensional harmonic oscillator, i.e., $V(x,t) = x^T M(t)x + \epsilon V_I(x,t)$, where $M(t) \in \mathbb{R}^{d\times d}$ is a positive-definite matrix and $\epsilon V_I(x,t)$ is a small perturbation. The real scalar function σ originates from the mean-field interaction between the particles and corresponds to repulsive or attractive forces for positive or negative values of $\sigma(t)$, respectively [5]. Notice that the noninteracting case, $\sigma \equiv 0$, corresponds to the linear Schrödinger equation.

Several methods have been analyzed to compute both the time evolution and the ground state of the GPE in the course of the past decade [1–3,6,7], among them finite differences, Galerkin spectral methods, and pseudospectral methods for Fourier or Hermite basis expansions. It has been concluded [2] that these pseudospectral methods perform best for a wide parameter range for the GPE. The Fourier-type methods can be implemented with fast Fourier transform (FFT) algorithms since the trapping potential V causes the wave function to vanish asymptotically, thus allowing us to consider the problem as periodic on a sufficiently large spatial interval. Their advantages are high accuracy with a moderate number of mesh points and low computational cost. For harmonic-oscillator (HO) problems, however, the exact solution is known, and by expanding the solution in Hermite polynomials, highly accurate results are obtained if the HO is solved separately [2,3,6,7].

It is claimed [2] that either Hermite or Fourier pseudospectral methods are the most efficient, with the choice depending on the particular parameter set. Motivated by these results, we show how both methods are combined to retain both the accuracy of the Hermite method and the speed of the Fourier transforms, i.e., to rewrite the Hermite method as a single simple pseudospectral Fourier scheme. We have found that this approximation performs, for the studied problem class, always equal to or better than the original Fourier method, and therefore has to compete with Hermite expansions only. Hermite schemes suffer from large computational costs when the number of basis terms in the expansions is altered along the integration or taken very large, which is the case for time-dependent trap frequencies $M(t)$ or strong nonlinearities $\sigma(t)$. It is in this setup where our method substantially improves the Hermite performance, and it can indeed be regarded as the optimal choice for the number of Hermite basis functions (for an equidistant grid) at each time step.

For ease of notation, we restrict ourselves to the one-dimensional problem

$$i\frac{\partial}{\partial t}\psi = H_0(t)\psi + [\varepsilon V_I(x,t) + \sigma(t)|\psi|^2]\psi, \qquad (1.1)$$

where

$$H_0(t) = \frac{1}{2\mu}p^2 + \frac{1}{2}\mu\omega^2(t)x^2 \qquad (1.2)$$

and $p = -i\frac{\partial}{\partial x}$. The boundary conditions imposed by the trap require the wave function to go to zero at infinity, and up to any desired accuracy we can assume $\psi(x,t)$ and all its derivatives to vanish outside a finite region, say $[a,b]$, which we divide using a mesh (usually with $N = 2^k$ points to allow a simple use of the FFT algorithms). Then, the partial differential equation (1.1) transforms into a system of ordinary differential equations (ODE's),

$$i\frac{d}{dt}u(t) = \hat{H}_0(t)u(t) + [\varepsilon V_I(X,t) + \sigma(t)|u(t)|^2]u(t), \qquad (1.3)$$

*phiba@imm.upv.es
†serblaza@imm.upv.es

and the harmonic part becomes

$$\hat{H}_0(t) = T + \tfrac{1}{2}\mu\omega^2(t)X^2, \tag{1.4}$$

with $u \in \mathbb{C}^N$, where $u_i(t) \simeq \psi(x_i,t)$, $x_i = a + ih$, $i = 0,1,\ldots,N-1$, $h = (b-a)/N$, $X = \mathrm{diag}\{x_0,\ldots,x_{N-1}\}$, and T denotes a discretization of the kinetic part.

This system of nonlinear ODE's can be numerically solved by standard all-purpose ODE methods. However, because of the particular structure of this problem, different numerical methods can differ considerably in accuracy as well as in computational cost and stability. In addition, the structural properties of the system lead to the existence of several preserved quantities such as the norm and energy (for the autonomous case).

The accurate preservation of these quantities as well as the error propagation and performance of splitting methods explain why they are frequently recommended for the time integration [2,3,6], and make them the subject of investigation in this work.

II. SPLITTING METHODS

Let us consider the separable system of ODE's,

$$u' = A(u) + B(u), \quad u(t_0) = u_0 \in \mathbb{C}^N, \tag{2.1}$$

where we assume that both systems

$$u' = A(u), \quad u' = B(u) \tag{2.2}$$

can either be solved in closed form or accurately integrated. If $\varphi_t^{[A]}$, $\varphi_t^{[B]}$ represent the exact flows associated with (2.2), then to advance the solution one time step, h, we can use, for example, the composition $\psi_h^{[1]} = \varphi_h^{[A]} \circ \varphi_h^{[B]}$ (i.e., $u(t_0+h) \simeq \psi_h^{[1]}(u_0) = \varphi_h^{[A]}[\varphi_h^{[B]}(u_0)]$), which is known as the first-order Lie-Trotter method. A method has order p if $\psi_h^{[p]} = \varphi_h + O(h^{p+1})$, where φ_t denotes the exact global flow of (2.1). Sequential application of the two first-order methods $\psi_h^{[1]}$ and its adjoint $\psi_h^{[1]*} = \varphi_h^{[B]} \circ \varphi_h^{[A]}$ with a half time step yields the second-order time-symmetric methods

$$\psi_{h,A}^{[2]} = \varphi_{h/2}^{[A]} \circ \varphi_h^{[B]} \circ \varphi_{h/2}^{[A]}, \tag{2.3}$$

$$\psi_{h,B}^{[2]} = \varphi_{h/2}^{[B]} \circ \varphi_h^{[A]} \circ \varphi_{h/2}^{[B]} \tag{2.4}$$

(referred to as ABA and BAB compositions). The contraction via the (one-parameter-) group property of the flows that eliminated one computation is called the first same as last (FSAL) property, and it can also be used with higher-order m-stage compositions

$$\psi_h^{[p]} = \varphi_{a_m h}^{[A]} \circ \varphi_{b_m h}^{[B]} \circ \cdots \circ \varphi_{a_1 h}^{[A]} \circ \varphi_{b_1 h}^{[B]} \tag{2.5}$$

if $a_m = 0$ or $b_m = 0$ and repeated application of the scheme without requiring output. For linear problems, it is usual to replace the flow maps by exponentials (for nonlinear problems, the same is possible using exponentials of Lie operators). In this notation, the equation $iu' = A(u) + B(u)$, whose formal solution for the evolution operator is denoted by $\phi_t^{[A+B]} = e^{-it(A+B)}$, is approximated for one time step, h, by the order p composition (2.5), or, equivalently,

$$\psi_h^{[p]} \equiv e^{-iha_m A} e^{-ihb_m B} \cdots e^{-iha_1 A} e^{-ihb_1 B}. \tag{2.6}$$

We keep in mind that, in a nonlinear problem, if B depends on u, it has to be updated at each stage because u changes during the evolution of $e^{-iha_i A}$.

There exist many different splitting methods that are designed for different purposes, depending on the structure of the problem, the desired order, the required stability, etc. [8–14].

When H_0 is the dominant part, it is worthwhile to take a closer look at the split (1.1). This would correspond to $\|B\| \ll \|A\|$, and for this case, when facing autonomous problems, there exist tailored methods that have shown a high performance in practice. Writing the equation as $iu' = (A + \epsilon B)u$ (with ϵ a small parameter), it is clear that the local error of the second-order methods (2.3) or (2.4) comes from the commutators at third order $[A,[A,\epsilon B]]$ and $[\epsilon B,[A,\epsilon B]]$, where $[A,B] := AB - BA$, and for simplicity, we have denoted $A = A(u)\cdot\nabla$, $B = B(u)\cdot\nabla$, and we can say that the local error is of order $O(\epsilon h^3 + \epsilon^2 h^3)$. The coefficients a_i, b_i in the general composition (2.6) can be chosen to cancel the dominant error terms, say, the $O(\epsilon h^r)$ terms for relatively large values of r. Then, one can denote the effective order of a method by (r,p) with $r \geqslant p$ when the local error is given by $O(\epsilon h^{r+1} + \epsilon^2 h^{p+1})$. The method is of order p, but in the limit $\epsilon \to 0$ it is considered to be of order $r \geqslant p$. Using this split allows us to gain a factor ϵ in accuracy even for general splitting methods where $r = p$. In [11], several methods of order $(r,2)$ for $r \leqslant 10$ are obtained with all coefficients a_i, b_i being positive, and some other schemes of order $(r,4)$ for $r = 6,8$ are presented. For near-integrable systems, these last methods are the most efficient and stable. Despite the gain of accuracy, the split into a dominant part and a small perturbation is left unconsidered when it leads to involved or computationally costly algorithms. This issue is addressed in this work.

To take into account the time dependence in the vector fields in (1.1), a more detailed analysis is required. For simplicity in the presentation, we consider a linear problem, but the same results are valid for a nonlinear problem. The general separable equation

$$iu' = A(t)u + \epsilon B(t)u, \tag{2.7}$$

with $|\epsilon| \ll 1$, can be solved by considering the time as two new independent coordinates

$$\begin{cases} iu' &= A(t_2)u \\ t_1' &= 1 \end{cases}, \qquad \begin{cases} iu' &= \epsilon B(t_1)u \\ t_2' &= 1 \end{cases}. \tag{2.8}$$

If we consider the symmetric second-order operator splitting method, we have

$$\phi_h = e^{-i\frac{h}{2}\epsilon B(t_n+h)} e^{-ihA(t_n+\frac{h}{2})} e^{-i\frac{h}{2}\epsilon B(t_n)} + O(h^3), \tag{2.9}$$

where ϕ_h denotes the exact evolution operator for one time step. Notice that the local error is not proportional to ϵ and this split does not take advantage of the near-integrability of the problem. This result is proved in [15], where it is shown that near-integrability is recovered if we take the time as a new variable as follows:

$$\begin{cases} iu' &= A(t_1)u \\ t_1' &= 1 \end{cases}, \qquad iu' = \epsilon B(t_1)u. \tag{2.10}$$

TABLE I. Algorithm for the numerical integration of the system (2.10) by the composition (2.5).

Algorithm for one time step $t_n \to t_n + h$	
$t^{[0]} = t_n$	
do $i = 1,m$	
$solve:\ u' = B(u,t^{[i-1]}),$	$t \in [t^{[i-1]}, t^{[i-1]} + b_i h]$
$solve:\ u' = A(u,t),$	$t \in [t^{[i-1]}, t^{[i-1]} + a_i h]$
$t^{[i]} = t^{[i-1]} + a_i h$	
enddo	
$t_{n+1} = t^{[m]}$	

The symmetric second-order operator splitting now reads

$$\phi_h = e^{-i\frac{h}{2}\epsilon B(t_n+h)} e^{-i\tilde{A}(t_n+h,t_n)} e^{-i\frac{h}{2}\epsilon B(t_n)} + O(\epsilon h^3), \quad (2.11)$$

where $\exp[-i\tilde{A}(t_n+h,t_n)]$ denotes the exact flow of the nonautonomous equation $iu' = A(t)u$ from t_n to $t_n + h$. Notice that the error is a factor ϵ more accurate, and thus considerably larger time steps can be used. This result was proved in [15] for separable systems of ODE's. However, it is also valid for nonautonomous separable operators in partial differential equations (PDE's), and we illustrate the performance of this split in numerical examples.

Both schemes (2.9) and (2.11) are time-symmetric, and higher-order methods can be easily obtained by composition or by extrapolation (multiproduct expansion). It is clear that much more accurate results are obtained by taking (2.11) as the basic method.

To build methods from low to moderate orders, however, it is more efficient to consider a composition method designed for near-integrable systems, following the scheme shown in Table I.

We show that the exact solution of the nonautonomous problem, in our setting the dominant part H_0 of (1.1),

$$i\frac{\partial}{\partial t}\psi = \left(\frac{1}{2\mu}p^2 + \frac{1}{2}\mu\omega^2(t)x^2\right)\psi, \quad (2.12)$$

is easily computed for a time step using Fourier transforms. Before giving the details on the time integration, some remarks on the formal solution are necessary.

It is well known that H_0 is an element of the Lie algebra spanned by the operators $\{E = x^2/2, F = p^2/2, G = \frac{1}{2}(px + xp)\}$, where $\mu = 1$ for simplicity, and its commutators are

$$[E,F] = iG, \quad [E,G] = 2iE, \quad [F,G] = -2iF.$$

This is a three-dimensional Lie algebra, and the solution, $\psi(x,t) = U(t,0)\psi(x,0)$, of (2.12) can be expressed as a single exponential using the Magnus series expansion [16,17] or as a product of exponentials [18]. It is possible to formulate the evolution operator $U(t,0)$ in many different ways, the most appropriate depending on the particular purpose, e.g., using the Magnus expansion

$$U(t,0) = \exp[f_1(t)E + f_2(t)F + f_3(t)G] \quad (2.13)$$

for certain functions $f_i(t)$ [19]. Approximations of (2.13) for one time step, h, on the other hand, are easily obtained, e.g., a fourth-order commutator-free method is given by [20]

$$U(t+h,t) = \exp\left[\frac{h}{2}\left(\frac{1}{2}p^2 + \omega_L^2\frac{1}{2}x^2\right)\right] \times \exp\left[\frac{h}{2}\left(\frac{1}{2}p^2 + \omega_R^2\frac{1}{2}x^2\right)\right] + O(h^5), \quad (2.14)$$

where

$$\omega_L^2 = \alpha\omega_1^2 + \beta\omega_2^2, \quad \omega_R^2 = \beta\omega_1^2 + \alpha\omega_2^2$$

with $\omega_i = \omega(t_n + c_i h)$, $c_1 = \frac{1}{2} - \frac{\sqrt{3}}{6}$, $c_2 = \frac{1}{2} + \frac{\sqrt{3}}{6}$, and $\alpha = \frac{1}{2} - \frac{1}{\sqrt{3}}$, $\beta = 1 - \alpha$. It can be considered as the composition of the evolution for half time step of two oscillators with averaged frequencies, using the fourth-order Gauss-Legendre quadrature points to evaluate $\omega(t)$. Different quadrature rules can also be used and correspond to different averages along the time step, see [17,20]. In the limit when ω is constant, the exact solution is recovered. Higher-order approximations are available, if more accurate results are desired, by approximating the functions f_i in (2.13) via truncated Magnus expansions.

Our objective is to obtain a factorization of the solution that only involves terms proportional to E or F since they are easy to compute, as we show in the following paragraph.

Starting from (2.14) or high-order approximates of (2.13), the main result of this work is the natural decomposition for the application of Fourier spectral methods.

A. Hamiltonians for spectral methods

We now analyze how to compute the evolution of different parts of the Hamiltonian by spectral methods. The spatial derivative (or kinetic part) associated with the semidiscretized problem (1.3) can be solved in the momentum space by noting that

$$e^{-itT}u = \mathcal{F}_N^{-1} e^{-itD_N}\mathcal{F}_N u,$$

where D_N is diagonal and $\mathcal{F}_N$ denotes the discrete Fourier transform of length N, whose computation can be accomplished by the FFT algorithm with $O(N\log N)$ floating point operations. The exponentials in e^{-ihD_N} need to be computed only once and can be reused at each step such that the cost of the action of e^{-ihD_N} corresponds to N complex products.

For the remaining part, the following well-known result is very useful:

Lemma II.1. If F is real-valued, the equation

$$i\frac{\partial}{\partial t}\phi(x,t) = F(x,|\phi(x,t)|)\phi(x,t) \quad (2.15)$$

leaves the norm invariant, $|\phi(x,t)| = |\phi(x,0)|$, and then

$$\phi(x,t) = e^{-itF(x,|\phi(x,0)|)}\phi(x,0). \quad (2.16)$$

On the other hand, it is well known that the solutions of the linear Schrödinger equation with the harmonic potential

$$i\frac{\partial}{\partial t}\phi(x,t) = \frac{1}{2}(p^2 + x^2)\phi(x,t) \quad (2.17)$$

can be expressed in terms of Hermite polynomials,

$$\phi(x,t) = \sum_{n=0}^{\infty} c_n e^{-iE_n t} h_n(x), \tag{2.18}$$

where

$$E_n = n + \frac{1}{2}, \qquad h_n(x) = \frac{1}{\pi^{1/4}\sqrt{2^n n!}} H_n(x) e^{-x^2/2} \tag{2.19}$$

and $H_n(x)$ are the Hermite polynomials. The weights c_n can be computed from the initial conditions, $c_n = \int h_n(x)\phi(x,0)\,dx$.

The previous results show how to compute individual parts of the equation and thus permit different ways of splitting the system in two solvable parts,

$$i\psi_t = (A + B)\psi. \tag{2.20}$$

We consider the following cases:

(i) Fourier (F) split:

$$A = \frac{1}{2}p^2, \quad B(t) = \frac{\omega(t)}{2}x^2 + \varepsilon V_I(x,t) + \sigma(t)|\psi|^2. \tag{2.21}$$

We take the time as a new coordinate, as in (2.10), and evolve it with A, which is now autonomous and exactly solvable, and freeze the time in B, which is then solved using the result from Lemma II.1. Here, A and B are diagonal in the momentum and coordinate spaces, respectively, and we can change between them using the Fourier transforms.

(ii) Harmonic oscillator (HO) split: Letting for a moment $\omega = 1$, the Hermite expansion then suggests a split,

$$A = \tfrac{1}{2}(p^2 + x^2), \qquad B(t) = \varepsilon V_I(x,t) + \sigma(t)|\psi|^2, \tag{2.22a}$$

where the solution for the equation $iu' = Au$ can be approximated using a finite number of Hermite basis functions, i.e.,

$$\phi_M(x,t) = \sum_{n=0}^{M-1} c_n e^{-iE_n t} h_n(x). \tag{2.22b}$$

Since B is diagonal in coordinate space, it will act as a simple multiplication if we choose a number of Hermite basis functions and evaluate them at the points of a chosen mesh (e.g., using the Gauss-Hermite quadrature [21] or on equidistant grid points [2]). This split can be of interest if all contributions from $B(t)$ are small with respect to A and methods for near-integrable systems are used. If the frequency is time-dependent, the corresponding split is

$$A(t) = \tfrac{1}{2}[p^2 + \omega^2(t)x^2], \quad B(t) = \varepsilon V_I(x,t) + \sigma(t)|\psi|^2. \tag{2.23}$$

In this case, it is convenient to take the time t as a new coordinate, as shown in (2.10). The solution of $iu' = A(t)u$, in the algorithm in Table I, can be approximated by the Magnus expansion, e.g., (2.13) or (2.14), but these factorizations are not appropriate for use with spectral methods since it would require two sets of basis functions and additional transformations.

In general, the split (i) can be considered faster and simpler since $A \equiv T$ can be computed in the momentum space, and one can easily and efficiently change from momentum to coordinate space via FFT's. The choice (ii), on the other hand, allows us to take advantage of the structure of a near-integrable system if, roughly speaking, $\|B\| < \|A\|$, but it requires us to solve the equation for the (time-dependent) harmonic potential exactly (or with high accuracy). The evolution of the constant oscillator is easily computed using Hermite polynomials (see [2,3,21]), but the evolution for the explicitly time-dependent problem is more involved.

B. Solving the harmonic oscillator by Fourier methods

We propose a method that combines the advantages of both splittings. It retains the advantages of the HO split (ii) while being as fast to compute as the F split in (i). For this purpose, we briefly review some basic concepts of Lie algebras.

Given X, Y as two elements of a given Lie algebra, it is well known that

$$e^X Y e^{-X} = Y + [X,Y] + \tfrac{1}{2}[X,[X,Y]] + \cdots.$$

Given $X(x), P(p)$ and an analytic function $F(x,p)$, we are interested in the following adjoint actions:

$$e^{-itX} F(x,p) e^{itX} = F(x, p + tX'), \tag{2.24a}$$
$$e^{-itP} F(x,p) e^{itP} = F(x - tP', p), \tag{2.24b}$$

where $X' = dX/dx$, $P' = dP/dp$. In classical mechanics, this corresponds to a kick and a drift.

As we have seen, the exponentials $\exp(\alpha x^2/2)$ and $\exp(\beta p^2/2)$ can be easily computed by Fourier spectral methods. It is then natural to ask whether it is possible to write the solution of (2.12) as a product of exponentials that are solvable by spectral methods. The answer is positive and it is formulated as follows.

Let us first consider the pure harmonic oscillator, whose result was obtained in [22], and for which we present a proof that applies equally to the general case.

Lemma II.2. Let $A_1 = \frac{1}{2}p^2$, $B_1 = \frac{1}{2}x^2$, and

$$g(t) = \sin(t), \quad f(t) = [1 - \cos(t)]/\sin(t). \tag{2.25}$$

Then, the following property is satisfied for $|t| < \pi$:

$$e^{-it(A_1+B_1)} = e^{-if(t)A_1}\, e^{-ig(t)B_1}\, e^{-if(t)A_1} \tag{2.26}$$
$$= e^{-if(t)B_1}\, e^{-ig(t)A_1}\, e^{-if(t)B_1}. \tag{2.27}$$

Proof. A constructive way to derive the functions f, g makes use of the parallelism with the one-dimensional classical harmonic oscillator with Hamiltonian $H = \frac{1}{2}p^2 + \frac{1}{2}q^2$ and Hamilton equations

$$\frac{d}{dt}\begin{Bmatrix} q \\ p \end{Bmatrix} = \begin{pmatrix} 0 & 1 \\ -1 & 0 \end{pmatrix}\begin{Bmatrix} q \\ p \end{Bmatrix} = (A + B)\begin{Bmatrix} q \\ p \end{Bmatrix}, \tag{2.28}$$

where

$$A \equiv \begin{pmatrix} 0 & 1 \\ 0 & 0 \end{pmatrix}, \qquad B \equiv \begin{pmatrix} 0 & 0 \\ -1 & 0 \end{pmatrix}. \tag{2.29}$$

The Lie algebra generated by the matrices A, B is the same as the Lie algebra associated with the operators A_1, B_1 for the Schrödinger equation with the harmonic potential (2.17).

The exact evolution operator of (2.28) is

$$O(t) = \begin{pmatrix} \cos(t) & \sin(t) \\ -\sin(t) & \cos(t) \end{pmatrix}, \tag{2.30}$$

which is an orthogonal and symplectic 2×2 matrix. For the splitted parts, the solutions are easily computed to

$$e^{f(t)A} = \begin{pmatrix} 1 & f(t) \\ 0 & 1 \end{pmatrix}, \qquad e^{g(t)B} = \begin{pmatrix} 1 & 0 \\ -g(t) & 1 \end{pmatrix}$$

and then, equating the symmetric composition

$$e^{fA} e^{gB} e^{fA} = \begin{pmatrix} 1 - fg & 2f - f^2 g \\ -g & 1 - fg \end{pmatrix}$$

to (2.30), we obtain (2.25), which is valid for $|t| \leqslant \pi$. The decomposition (2.27) is derived analogously. Using the Baker-Campbell-Haussdorf-formula, it is clear that both results remain valid, up to the first singularity at $t = \pm\pi$, when replacing the matrices A, B by the corresponding linear operators A_1, B_1, since all computations are done in identical Lie algebras.

Given the functions f, g, we can prove the lemma directly by recalling that two operators are identical on a sufficiently small time interval if they satisfy the same first-order differential equation with the same initial conditions [23]. We thus verify that the right-hand side of (2.26) also solves the propagator equation

$$iU' = (A_1 + B_1)U, \qquad U(0) = I \tag{2.31}$$

and is therefore identical to the propagator on the left-hand side. Now setting

$$\tilde{U}(t) = e^{-if(t)A_1} e^{-ig(t)B_1} e^{-if(t)A_1}$$

and plugging it into (2.31) yields

$$\begin{aligned}(A_1 + B_1)\tilde{U} \stackrel{!}{=} (&\dot{f} A_1 + e^{-if A_1}\, \dot{g} B_1\, e^{if A_1} \\ &+ e^{-if A_1}\, e^{-ig B_1}\, \dot{f} A_1\, e^{ig B_1}\, e^{if A_1})\tilde{U}.\end{aligned}$$

Using (2.24a) and (2.24b), we obtain two independent nonlinear differential equations for $f(t)$ and $g(t)$ with initial condition $f(0) = g(0) = 0$ to satisfy $\tilde{U}(0) = I$. It is then easy to check that f, g given in (2.25) solve these equations. As a result, we have that $\tilde{U}(t) = U(t)$ locally in a neighborhood of the origin and (2.27) is proved identically.

For practical purposes, the singularities occur at sufficiently large times and hence do not impose limits for the time steps of numerical methods.

It is immediate to generalize this result to the equation

$$i\frac{\partial}{\partial t}\psi(x,t) = \left(\frac{1}{2\mu}p^2 + \mu\frac{\omega^2}{2}x^2\right)\psi(x,t),$$

$\mu, \omega > 0$ by replacing (2.25) with

$$g = \frac{1}{\mu\omega}\sin(\omega t), \quad f = \mu\omega\frac{1 - \cos(\omega t)}{\sin(\omega t)}.$$

This result is valid for $|t| < t^* \equiv \pi/\omega$.

The following theorems extend this idea to decompositions of operators that appear after the approximation of the time-dependent parts via (2.13) or by the composition (2.14).

Theorem II.3. Let α, β, γ be constants, $\eta = \sqrt{\alpha\gamma - \beta^2}$, and

$$\begin{aligned} g(t) &= \gamma/\eta\, \sin(\eta t), \\ f(t) &= \frac{1}{g(t)}\left(1 - \cos(\eta t) + \frac{\beta}{\eta}\sin(\eta t)\right), \\ e(t) &= \frac{1}{g(t)}\left(1 - \cos(\eta t) - \frac{\beta}{\eta}\sin(\eta t)\right). \end{aligned} \tag{2.32}$$

Then, the following decomposition holds for $0 \leqslant t < \pi/\eta$:

$$e^{-i\frac{t}{2}[\alpha x^2 + \beta(xp+px) + \gamma p^2]} = e^{-if(t)\frac{1}{2}x^2}\, e^{-ig(t)\frac{1}{2}p^2}\, e^{-ie(t)\frac{1}{2}x^2}. \tag{2.33}$$

Proof. The proof follows the lines of the proof of Lemma II.2. The evolution operator associated with the classical Hamiltonian $H = \frac{1}{2}(\alpha x^2 + 2\beta xp + \gamma p^2)$ is given by

$$\begin{pmatrix} \cos(\eta t) + \frac{\beta}{\eta}\sin(\eta t) & \frac{\gamma}{\eta}\sin(\eta t) \\ -\frac{\alpha}{\eta}\sin(\eta t) & \cos(\eta t) - \frac{\beta}{\eta}\sin(\eta t) \end{pmatrix}, \tag{2.34}$$

and equality to the right-hand side of (2.33) is verified by straightforward computation of the matrix exponentials. The solution is valid until the first singularity at $t = \pi/\eta$. Using (2.24a) and (2.24b), it can be checked that both sides of (2.33) satisfy the same differential equation and initial conditions. Now, the initial conditions become $f(0) = -e(0), g(0) = 0$ because the loss of symmetry in the decomposition has to be taken into account.

Theorem II.4. Let $\omega_k \in \mathbb{R}$, $c_k = \cos(\omega_k t/2)$, $s_k = \sin(\omega_k t/2)$ for $k = L, R$, and

$$\begin{aligned} g(t) &= s_L c_R/\omega_L + c_L s_R/\omega_R, \\ f(t) &= \frac{1}{g(t)}\left(1 - c_L c_R + \frac{\omega_L}{\omega_R} s_L s_R\right), \\ e(t) &= \frac{1}{g(t)}\left(1 - c_L c_R + \frac{\omega_R}{\omega_L} s_L s_R\right). \end{aligned} \tag{2.35}$$

Then, the decomposition

$$\begin{aligned} &e^{-i\frac{t}{2}(\frac{1}{2}p^2 + \omega_L^2\frac{1}{2}x^2)} e^{-i\frac{t}{2}(\frac{1}{2}p^2 + \omega_R^2\frac{1}{2}x^2)} \\ &\quad = e^{-if(t)\frac{1}{2}x^2} e^{-ig(t)\frac{1}{2}p^2} e^{-ie(t)\frac{1}{2}x^2} \end{aligned} \tag{2.36}$$

is satisfied for $0 \leqslant t < t^*$, where t^* is the smallest positive root of $g(t)$.

The proof is similar to the previous one.

III. THE HERMITE-FOURIER METHODS

With the presented exact decompositions at hand, we now solve the discretized GPE (1.3) by splitting methods using the symmetric compositions (2.3) and (2.4). Let us first consider the case $\omega = 1$ and take the HO split $A = A_1 + B_1$,

$$\psi_{h,A}^{[2]} = e^{-ih(A_1+B_1)/2}\, e^{-ihB}\, e^{-ih(A_1+B_1)/2}, \tag{3.1}$$

$$\psi_{h,B}^{[2]} = e^{-ihB/2}\, e^{-ih(A_1+B_1)}\, e^{-ihB/2}. \tag{3.2}$$

Replacing the exponentials $e^{-ih(A_1+B_1)}$ by (2.26) or (2.27), we obtain four different methods whose computational costs differ considerably. At first glance, using the FSAL property, both (3.1) and (3.2) are equivalent from a computational point of view and require one exponential of B and another of $A_1 + B_1$

per step. However, a significant difference arises when we plug in the decompositions (2.26) or (2.27). Only the combination (3.2) with (2.27) yields a method that involves only one FFT and one inverse FFT call per step

$$\begin{aligned}\psi_h^{[2]} &= e^{-ihB/2}e^{-ih(A_1+B_1)}e^{-ihB/2}\\ &= e^{-ihB/2}e^{-if(h)B_1}e^{-ig(h)A_1}e^{-if(h)B_1}e^{-ihB/2}\\ &= e^{-i(hB/2+f(h)B_1)}e^{-ig(h)A_1}e^{-i(hB/2+f(h)B_1)}\end{aligned} \tag{3.3}$$

and solves exactly the harmonic oscillator for $|h| < h^*$. For any other combination, more kinetic terms have to be computed per step since the FSAL property cannot be exploited to the full extent, and this results in more costly [24] methods for the same accuracy.

The general composition (2.6) can be rewritten in the same way by replacing each flow e^{-ia_iA} in (2.6) by the composition (2.27)

$$\begin{aligned}\Phi_h \equiv\ & e^{-i(hb_mB+\alpha_mB_1)}\,e^{-ig(a_mh)A_1}\,e^{-i(hb_mB+\alpha_{m-1}B_1)}\cdots\\ &\times e^{-i(hb_1B+\alpha_1B_1)}\,e^{-ig(a_1h)A_1}\,e^{-i\alpha_0B_1},\end{aligned} \tag{3.4}$$

where $\alpha_k = f(a_{k+1}h) + f(a_kh)$, $k = 0,1,\ldots,m+1$ with $a_0 = a_{m+1} = 0$. This method is valid for $|a_ih| < h^*$, $i = 1,\ldots,m$ and requires only m calls of the FFT and its inverse, but reaches the same accuracy as if the Hermite functions were used.

In the more general case with a time-dependent frequency, $\omega(t)$, starting from the HO splitting, the time-dependent part is first approximated by Magnus expansions (2.13) or (2.14). Theorems II.3 and II.4 then provide decompositions to write the product of exponentials in a similar way as in (3.4), but now $\alpha_k = f(a_{k+1}h) + e(a_kh)$ and it is valid for $|a_ih| < t^*$, $i = 1,\ldots,m$, where t^* is the first zero of $g(t)$. At each stage, one has to compute $f(a_ih), g(a_ih), e(a_ih)$ from $\omega(t)$.

As in the previous case, it only requires m calls of the FFT and its inverse, like the standard Fourier pseudospectral methods. For stability reasons, it seems convenient to look for splitting methods whose value of $\max_i\{|a_i|\}$ is as small as possible.

IV. NUMERICAL EXAMPLES

We analyze first the performance of the methods considered in this work for the one-dimensional problem (1.1) with $\mu = \omega^2 = 1$, and the pure harmonic trap, i.e., $V_I = 0$.

To illustrate the validity of the decomposition presented in Lemma II.2, we first consider the linear problem ($\sigma = 0$). We take the ground state at $t = 0$ as an initial condition whose exact solution is given by

$$\psi(x,t) = \frac{1}{\pi^{1/4}}e^{-it/2}e^{-x^2/2}.$$

We discretize on the interval $[-10,10]$ to ensure the wave function and its first derivatives vanish up to round off at the boundaries, and sample it at $N = 1024$ equidistant grid points. We integrate, with only one time step, from $t = 0$ to T for $T \in [-\pi,\pi]$, i.e., forward and backward in time. We measure the integrated error in the wave function, $\|u_{\rm ex}(T) - u_a(T)\|_2$, where $u_a(T)$ denotes the approximate numerical solution obtained using the split (2.27), and $u_{\rm ex}(T)$ is the exact solution at the discretized mesh. The result of this comparison is

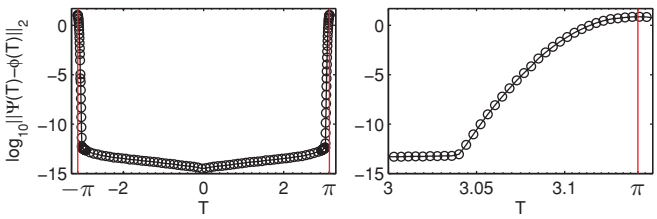

FIG. 1. (Color online) Error in logarithmic scale for the integration of the ground state of the harmonic potential using the split (2.27) for $T \in [-\pi,\pi]$ (integration forward and backward in time). The left and right panels show the 2-norm error and a zoom about $T = \pi$, respectively.

illustrated in Fig. 1 (left). The split (2.27) reproduces, for $|T| < \pi$, the exact solution up to round off, as expected. The right panel in Fig. 1 displays a zoom near a singularity where the error grows rapidly due to double-precision arithmetic.

We analyze how the approximation properties of the Hermite decomposition (2.22b) strongly depend on the function in question and on the chosen number of basis functions, M. We compute the M required to reach round-off precision for the evolution of a displaced ground state as an initial condition, $\psi_\delta(x,0) = e^{-(x-\delta)^2/2}/\pi^{1/4}$ from $t = 0$ to $T = 10$ in one time step. From initial conditions computed on a mesh, this can be accomplished as follows [2]:

$$u_{ex}(T) = e^{-iT(A_1+B_1)}u_0 \sim K^T e^{-iTD_1}K\,u_0, \tag{4.1}$$

where $D_1 = \mathrm{diag}\{\frac{1}{2},\frac{3}{2},\ldots,\frac{2M-1}{2}\}$, M is the number of basis elements considered, and $K_{i,j} = h_{i-1}(x_j)$, $i = 1,\ldots,M$, $j = 1,\ldots,N = 512$ with $h_n(x)$ given in (2.18), $x \in [-10,10]$. For $\delta = \frac{1}{10}$, round-off accuracy is achieved with $M = 8$, while for $\delta = 2$ it is necessary to take $M = 29$. We observe that the Hermite decomposition is very sensitive to the initial conditions [21]. The Hermite basis works efficiently as far as the initial conditions as well as the evolution thereof can be accurately approximated using a few number of basis elements, and one has to keep in mind that, for nonlinear problems, the number of basis functions necessary to reach a given accuracy can vary along the time integration.

Next, we study the following values for the nonlinearity parameter: $\sigma = 10^{-2},1,10^2$. The case $\sigma = 10^{-2}$ illustrates the performance of the proposed methods if applied to problems (linear or nonlinear) that are small perturbations of the harmonic potential, whereas the values $\sigma = 1,10^2$ are large enough to demonstrate the nonlinearity effects on the approximation properties of the methods. Physically, σ is proportional to the number of particles in a Bose-Einstein condensate and to the interaction strength [5].

For all cases, we choose the initial condition $\psi(x,0) = \rho e^{-(x-1)^2/2}$, with ρ a normalizing constant. We show in Fig. 2 the value of $|\psi(x,t)|^2$ at the initial and final time. The spatial interval is adjusted to ensure the wave function vanishes (up to round off) at the boundaries, here $[-20,20]$ for $\sigma = 0.01$ and $[-30,30]$ for both $\sigma = 1$ and 100, where the wave function moves faster (we only show the interval $x \in [-5,5]$). One can appreciate that for strong nonlinearities, the wave function can penetrate the potential barrier considerably, and one expects that an accurate approximation of these wave

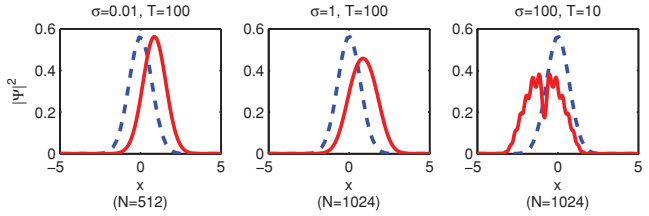

FIG. 2. (Color online) Exact evolution at $t = T$ (solid red line) from the initial conditions given by $\psi(x,0) = \rho e^{-(x-1)^2/2}$ (dashed blue line). The number of grid points is given by N.

functions requires a large number of Hermite functions when using (4.1), which renders this procedure inappropriate.

A. HO split versus F split

We analyze now the advantages of the HO split versus the F split as given in (2.23) and (2.21).

In a first experiment, we fix the symmetric second-order BAB composition (3.2) and apply it for both splits. For the HO split, we compute the harmonic part either with the decomposition (2.27) or in the Hermite basis (4.1) with different numbers of basis terms.

The parameters, initial conditions, and final times are taken as previously for Fig. 2. Given a splitting method X, we denote by X_F, X_H, and $X_H M$ its implementations with the F split, the HO split using the Hermite-Fourier method, and the HO split using M Hermite basis functions in (4.1), respectively. We measure the error versus the number of exponentials that can be considered proportional to the computational cost, and we plot the results in Fig. 3. As expected, HO splits are advantageous if the system is close to a harmonic oscillator, i.e., for $\sigma = 0.01, 1$, and if the initial conditions are accurately approximated by a few terms in the Hermite expansion. On the other hand, for strong nonlinearities $\sigma = 100$, the Hermite polynomial-based HO split shows a poor performance, cf. the large number of basis terms in the right panel of Fig. 3. We stress that if this technique is used for nonlinearities, the number of basis terms should be increased along the time integration, and fixing it bounds the maximally achievable accuracy and its limit depends on the initial condition and the strength of the nonlinearity.

The Hermite-Fourier method proposed in this work [using the composition (2.27)] is clearly superior for weak perturbations, and it maintains a similar performance to the F split for strong nonlinearities.

Finally, we analyze the performance of different higher-order splitting methods, which are useful when high accuracies are desired. The following methods (whose coefficients are collected in Table II for the convenience of the reader) are considered:

(i) RKN64 [the six-stage fourth-order method from [9]]. This is a partitioned Runge-Kutta-Nyström method and it is designed for the case in which $[B,[B,[B,A]]] = 0$, being the case for both the F split and the HO split.

(ii) NI(8,2) [the four-stage (8,2) BAB method from [11]]. This method is addressed to perturbed systems. One expects a high performance if the contribution from B is small.

(iii) NI(8,4) [the five-stage (8,4) BAB method from [11]].

TABLE II. Coefficients for several splitting methods.

The six-stage fourth-order: RKN64	
$b_1 = 0.082\,984\,406\,417\,4052$	$a_1 = 0.245\,298\,957\,184\,271$
$b_2 = 0.396\,309\,801\,498\,368$	$a_2 = 0.604\,872\,665\,711\,080$
$b_3 = -0.039\,056\,304\,922\,348\,6$	$a_3 = 1/2 - (a_1 + a_2)$
$b_4 = 1 - 2(b_1 + b_2 + b_3)$	$a_4 = a_3$, $a_5 = a_2$, $a_6 = a_1$
$b_5 = b_3$, $b_6 = b_2$, $b_7 = b_1$	
The four-stage (8,2) method: NI4	
$b_1 = 1/20$	$a_1 = 1/2 - \sqrt{3/28}$
$b_2 = 49/18$	$a_2 = 1/2 - a_1$
$b_3 = 1 - 2(b_1 + b_2)$	$a_3 = a_2$, $a_4 = a_1$
$b_4 = b_2$, $b_5 = b_1$	
The five-stage (8,4) method: NI5	
$b_1 = 0.811\,862\,738\,544\,516$	$a_1 = -0.007\,586\,913\,118\,774\,47$
$b_2 = -0.677\,480\,399\,532\,169$	$a_2 = 0.317\,218\,277\,973\,169$
$b_3 = 1/2 - (b_1 + b_2)$	$a_3 = 1 - 2(a_1 + a_2)$
$b_4 = b_3$, $b_5 = b_2$, $b_6 = b_1$	$a_4 = a_2$, $a_5 = a_1$

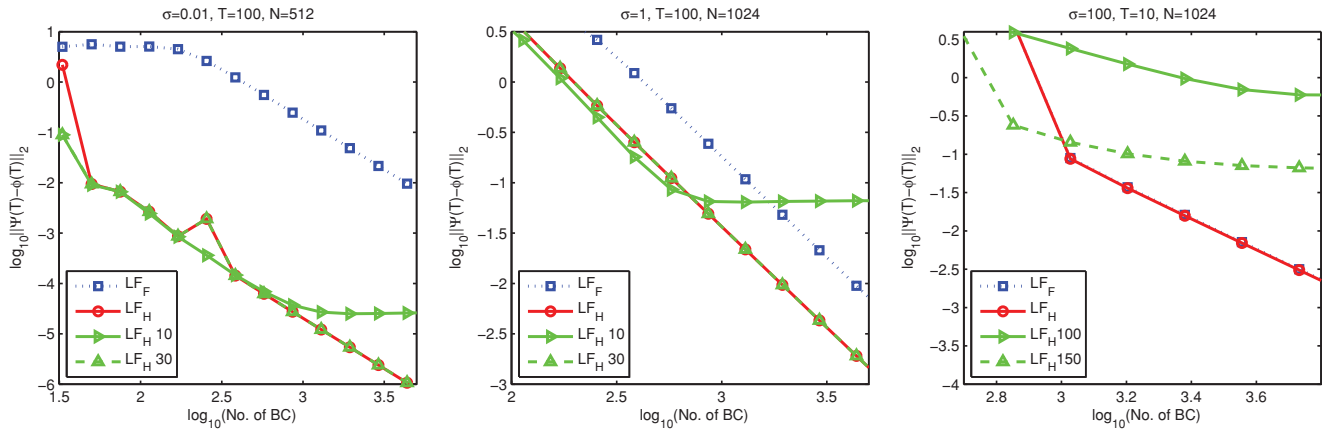

FIG. 3. (Color online) Error vs the number of basis changes (BC), i.e., Fourier or Hermite transforms, in logarithmic scale for different splittings for the leapfrog method (2.4).

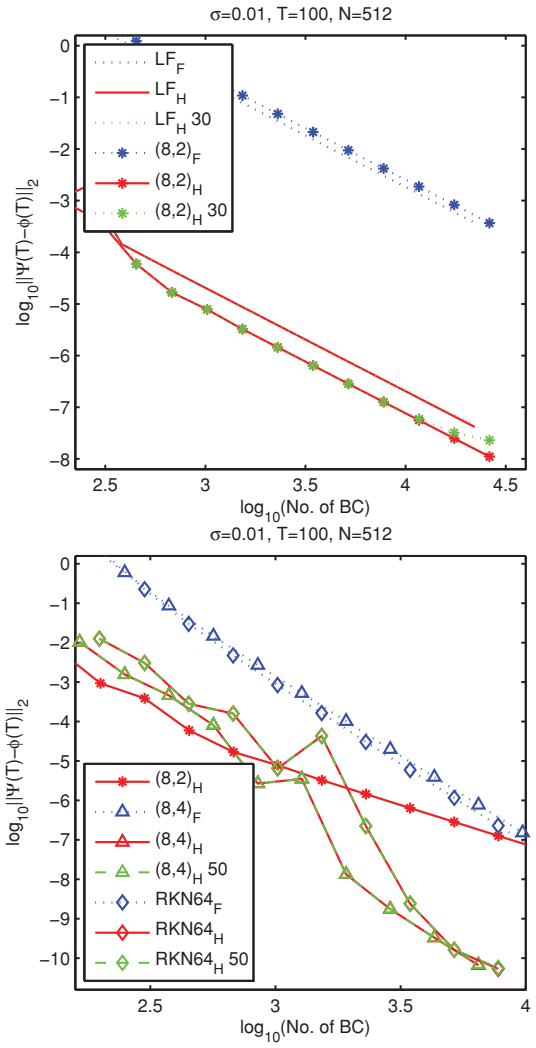

FIG. 4. (Color online) Comparison of second-order (upper panel) and fourth-order (lower panel) methods for the different splittings and decompositions discussed in the text and $\sigma = 0.01$. The curves for LF_H and $\mathrm{LF}_H 30$ overlap in the lower panel; the dashed curves are identical with the solid ones that correspond to the same composition method X, i.e., X_H overlaps with $X_H 50$.

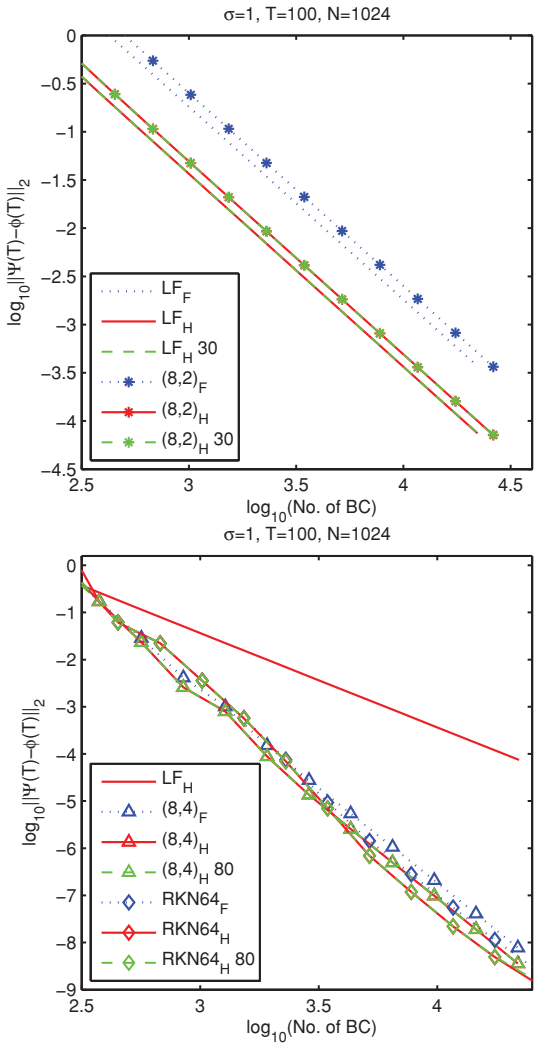

FIG. 5. (Color online) Same as Fig. 4 for $\sigma = 1$. In the upper panel, LF_H and $(8,2)_H$ coincide with $\mathrm{LF}_H 30$ and $(8,2)_H 30$, respectively.

We analyze in Figs. 4–6 the three problems specified in Fig. 3. In the upper panels, the leapfrog methods (LF) are compared with the second-order NI(8,2) methods. In the lower panels, we compare the RKN64 methods against the (8,4) methods jointly with the best among the previous second-order methods.

For a weak nonlinearity, when the system can be considered as a perturbed harmonic oscillator, we clearly observe that the HO split is superior to the F split. In this case, with a relatively small number of Hermite functions, it is possible to approach accurately the solution, but this procedure has a limited accuracy that can deteriorate along the time integration and depends on the initial conditions. In addition, the methods addressed to perturbed problems show the best performance: The $(8,2)_H$ method performs best among the compared methods when a relatively low accuracy is desired and the $(8,4)_H$ method takes its place for higher accuracies.

Figure 5 shows the results for $\sigma = 1$. It is qualitatively similar to the previous case, yet the HO split does not outperform the plain F split (2.21) as significantly as before. Nevertheless, it is important to observe that, again, the best result is obtained for the HO split. Notice that a higher number of Hermite basis functions is necessary to achieve the same accuracy as the Hermite-Fourier decomposition.

Figure 6 shows the results for $\sigma = 100$. The HO split cannot be expected to be particularly useful because the system is far from being a harmonic oscillator. From Fig. 2, we expect a great number of Hermite basis functions to be required for a sufficiently accurate expansion. The results in Fig. 6 demonstrate this rather intuitive expectation, i.e., almost negligible precision despite the large number of basis terms $M = 150$. Remarkably, the proposed HO decomposition does not show these limitations and reaches the precision of the F split (2.21) because we are solving the harmonic potential exactly up to spectral accuracy. For this problem, we observe that the LF method has the best performance when a relatively low accuracy is desired, the (8,4) method shows the best

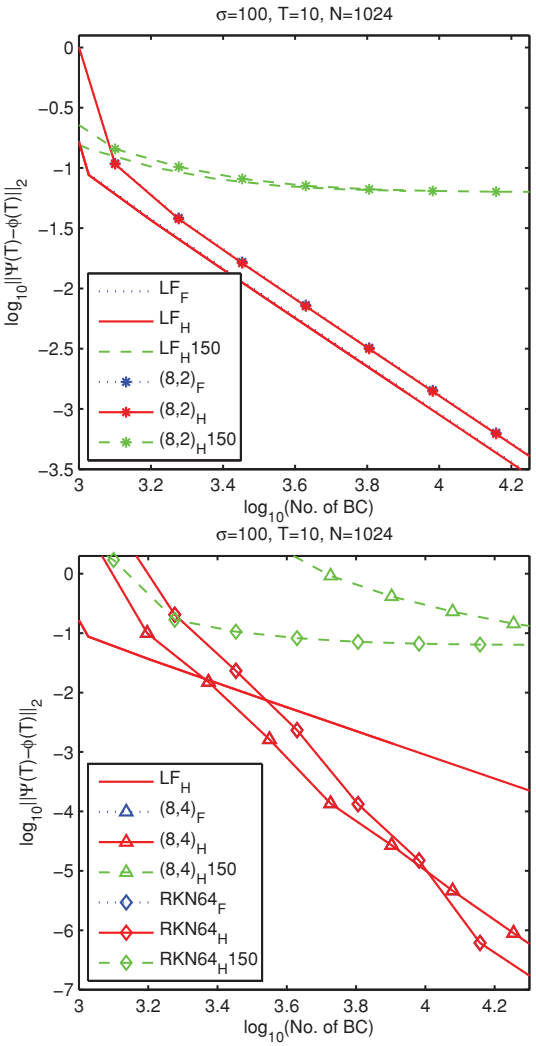

FIG. 6. (Color online) Same as Fig. 4 for $\sigma = 100$. F splittings (blue dashed) overlap the corresponding (solid red) Fourier-Hermite curves.

performance for medium accuracies, and the RKN64 is the method of choice for higher accuracies.

B. Time-dependent harmonic oscillator perturbed by weak quartic anharmonicity

We consider now a harmonic oscillator with time-dependent frequency and perturbed by a weak static quartic anharmonicity,

$$i\frac{\partial}{\partial t}\psi = \left(\frac{1}{2}p^2 + \frac{1}{2}\omega^2(t)x^2\right)\psi + \varepsilon_Q\frac{1}{4}x^4\psi. \qquad (4.2)$$

We first consider the case $\omega^2(t) = A[1+\epsilon\cos(wt)]$ with $w = 1/2$, $A = 4$, $\epsilon = 0.1$, $\varepsilon_Q = 0.01$. As reference, we take a highly accurate numerical approximation as the exact solution and restrict the spatial domain to $[-20,20]$ for all experiments in this subsection. We compare the Hermite-Fourier method with the plain Fourier split, since Hermite polynomials are not appropriate in a time-dependent setting. For fast oscillating systems and if high accuracy is needed, the two-exponential fourth-order approximation of the harmonic oscillator (2.14) can be improved by taking, for example, a higher-order Magnus expansion (2.13). As we have seen, the solution of

$$iU' = \left(\frac{1}{2}p^2 + \frac{1}{2}\omega^2(t)x^2\right)U \qquad (4.3)$$

can be written as

$$U(t,0) = e^{-i\frac{t}{2}[\alpha x^2+\beta(xp+px)+\gamma p^2]}, \qquad (4.4)$$

and we have considered, for example, a sixth-order Magnus integrator [17] to approximate the evolution operator for one fractional time step, $a_i h$, i.e., $U(t,t+a_i h)$. This is equivalent to taking in (4.4) $t = a_i h$, and the parameters α,β,γ are given by

$$\alpha = \frac{1}{18}(5\omega_1 + 8\omega_2 + 5\omega_3) + \frac{(a_i h)^2}{486} \times\left[\frac{17}{4}(\omega_1^2+\omega_3^2) + 8\omega_2^2 + \omega_1\omega_2 + \omega_2\omega_3 - \frac{37}{2}\omega_1\omega_3\right],$$

$$\beta = a_i h\sqrt{\frac{5}{3}}(\omega_3-\omega_1)\left[\frac{1}{12} + \frac{(a_i h)^2}{3240}(5\omega_1+8\omega_2+5\omega_3)\right],$$

$$\gamma = 1 + \frac{(a_i h)^2}{54}(\omega_1 - 2\omega_2 + \omega_3)$$

with $\omega_i = \omega(t_n + c_i h)$, $i = 1,2,3$, and $c_1 = 1/2 - \sqrt{15}/10$, $c_2 = 1/2$, $c_3 = 1/2 + \sqrt{15}/10$, corresponding to a sixth-order Gaussian quadrature rule. The obtained operator is then decomposed according to Theorem II.3.

The results are given in Fig. 7 and corroborate the superiority of the HO split.

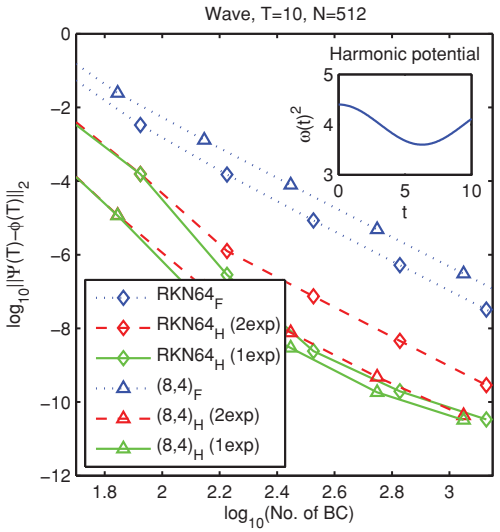

FIG. 7. (Color online) Comparison of Fourier and Fourier-Hermite splittings for two fourth order methods. The (red) dashed line indicates the two-exponential approximation (2.14), the (green) solid line corresponds to the sixth-order Magnus approximation presented in the text (4.4). The inset shows the evolution of the harmonic trap frequency $\omega(t)^2$ and the parameters used for the Hamiltonian are $w = 1/2$, $A = 4$, $\epsilon = 0.1$, $\varepsilon_Q = 0.01$.

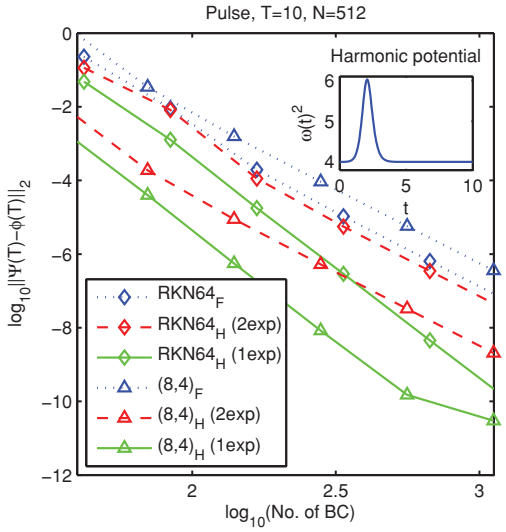

FIG. 8. (Color online) Compare Fig. 7. The parameters used are $w_0 = 4$, $A = 0.25$, and $B = 2$ with a small anharmonicity $\varepsilon_Q = 0.01$.

Another interesting example is given by an intense short pulse modeled via

$$\omega(t) = w_0 \left(1 + \frac{At}{\cosh^2[B(t-2)]}\right).$$

Varying the parameters A and B, the pulse can be sharpened while keeping its time average and hence its strength relative to the anharmonicity constant. Figure 8 shows the results obtained for a relatively slow variation of the harmonic potential, for the parameters $w_0 = 4$, $A = 0.25$, $B = 2$. Again, the advantageousness of the presented decomposition can be appreciated. It is already noticeable that the error introduced by the time dependence becomes dominant, and this effect increases for more rapidly varying potentials, e.g., for $B \gg 1$. In that case, higher-order approximations of the Magnus expansion are necessary to maintain the benefits of the Hermite composition.

V. CONCLUSIONS

We have presented Fourier methods for the numerical integration of perturbations of the time-dependent harmonic oscillator that are useful for both the Gross-Pitaevskii equation as well as for the linear Schrödinger equation. Fourier methods have shown a high performance in solving many different problems, which can be split into the kinetic part and a remainder that is diagonal in the coordinate space. We have extended the Fourier methods to perturbations of the time-dependent harmonic potential, and we refer to them as Hermite-Fourier methods. They solve the linear Schrödinger equation with a time-dependent harmonic potential to the desired order using corresponding Magnus expansions and up to the accuracy given by the spatial discretization. These methods are fast to compute since FFT's can be applied and show a high accuracy when the problem is a small perturbation of the harmonic potential. The methods presented in this work extend to perturbed harmonic potentials in linear quantum mechanics, cf. Sec. IV B, where it is straightforward to generalize the results to higher dimensions.

ACKNOWLEDGMENTS

We would like to acknowledge the referees for their careful reading and suggestions. The authors acknowledge the support of the Generalitat Valenciana through the project GV/2009/032. The work of S.B. has also been partially supported by Ministerio de Ciencia e Innovación (Spain) under the coordinated project MTM2010-18246-C03 (cofinanced by the ERDF of the European Union).

[1] W. Bao, D. Jaksch, and P. Markowich, J. Comput. Phys. **187**, 318 (2003).
[2] V. M. Pérez-García and X. Liu, Appl. Math. Comp. **144**, 215 (2003).
[3] M. Thalhammer, M. Caliari, and C. Neuhauser, J. Comput. Phys. **228**, 822 (2009).
[4] M. H. Anderson, J. R. Ensher, M. R. Matthews, C. E. Wieman, and E. A. Cornell, Science **269**, 198 (1995); C. C. Bradley, C. A. Sackett, J. J. Tollett, and R. G. Hulet, Phys. Rev. Lett. **75**, 1687 (1995); K. B. Davis, M.-O. Mewes, M. R. Andrews, N. J. van Druten, D. S. Durfee, D. M. Kurn, and W. Ketterle, *ibid.* **75**, 3969 (1995).
[5] C. J. Pethick and H. Smith, *Bose-Einstein Condensation in Dilute Gases* (Cambridge University Press, Cambridge, 2001).
[6] W. Bao, J. Shen, SIAM J. Sci. Comput. **26**, 2010 (2005).
[7] C. M. Dion and E. Cancés, Phys. Rev. E **67**, 046706 (2003).
[8] S. Blanes, F. Casas, and A. Murua, Bol. Soc. Esp. Mat. Apl. **45**, 89 (2008).
[9] S. Blanes and P. C. Moan, J. Comput. Appl. Math. **142**, 313 (2002).
[10] E. Hairer, C. Lubich, and G. Wanner, *Geometric Numerical Integration. Structure-Preserving Algorithms for Ordinary Differential Equations*, Springer Series in Computational Mathematics Vol. 31 (Springer-Verlag, Berlin, 2002).
[11] R. I. McLachlan, BIT **35**, 258 (1995).
[12] R. I. McLachlan and R. Quispel, Acta Numerica **11**, 341 (2002).
[13] M. Suzuki, Phys. Lett. A **146**, 319 (1990).
[14] H. Yoshida, Phys. Lett. A **150**, 262 (1990).
[15] S. Blanes, F. Diele, C. Marangi, and S. Ragni, J. Comput. Appl. Math. **235**, 646 (2010).
[16] W. Magnus, Commun. Pure Appl. Math. **7**, 649 (1954).
[17] S. Blanes, F. Casas, J. A. Oteo, and J. Ros, Phys. Rep. **470**, 151 (2009).
[18] J. Wei and E. Norman, J. Math. Phys. **4**, 575 (1963).
[19] Since F, G, E form a basis of the Lie algebra of the problem, there exist functions $f_i(t)$ that correspond to the summation of the Magnus series. The functions can be obtained by solving a set of differential equations; cf. [23].

[20] S. Blanes and P. C. Moan, Phys. Lett. A **265**, 35 (2000).
[21] C. Lubich, *From Quantum to Classical Molecular Dynamics: Reduced Models and Numerical Analysis*, Zurich Lectures in Advanced Mathematics (European Mathematical Society, Zürich, 2008).
[22] S. A. Chin and E. Krotscheck, Phys. Rev. E **72**, 036705 (2005).
[23] R. M. Wilcox, J. Math. Phys. **8**, 962 (1967).
[24] More precisely, the computational costs are due to a change of coordinates realized by the Fourier transform, which for this type of problem is equivalent to the number of kinetic terms.